

Hybrid Ligand Engineering for CdSe/CdS Core/Shell Colloidal Nanoplatelets

Abstract

Colloidal semiconductor nanoplatelets (NPLs) are attractive materials for optoelectronic applications due to their narrow emission linewidths, suppressed Auger recombination and directional emission characteristics. However, the long-chain organic ligands commonly used during synthesis act as insulating barriers, limiting charge transport and compromising device performance. In this work, we develop a hybrid ligand strategy for CdSe/CdS core/shell NPLs that combines inorganic metal halide passivation with organic alkyl amine ligands. In-solution ligand exchange with various metal halide salts enables efficient removal of native oleic acid ligands while preserving the optical and structural integrity of the NPLs. Among the investigated ligands, $(\text{NH}_4)_2\text{ZnCl}_4$ provides the most effective inorganic passivation, yielding the highest photoluminescence quantum yield (PLQY) among halide-treated samples (15%). Subsequent alkyl amine treatment restores colloidal stability in nonpolar solvents and leads to a substantial recovery of PLQY (60%), approaching that of the as-synthesized NPLs. This hybrid ligand approach offers an effective route toward simultaneously achieving compact surface passivation, high PLQY, and solution processability in colloidal NPLs.

Keywords: Colloidal semiconductor nanocrystals, Colloidal nanoplatelets, Ligand exchange, Optoelectronic materials, Inorganic ligands



CdSe/CdS Çekirdek/Kabuk Kolloidal Nanolevhacıklar için Hibrit Ligand Mühendisliği

Öz

[Kolloidal yarıiletken nanolevhacıklar (NPL'ler), dar ışımaya bant aralıkları, baskılanmış Auger birleşimi ve yönelimli ışımaya özellikleri sayesinde optoelektronik uygulamalar için oldukça cazip malzemelerdir. Ancak, sentez sırasında yaygın olarak kullanılan uzun zincirli organik ligandlar, yalıtkan bariyer olarak davranarak yük taşımamını sınırlar ve aygıt performansını olumsuz etkiler. Bu çalışmada, CdSe/CdS çekirdek/kabuk NPL'ler için inorganik metal halojenür pasivasyonu ile organik alkil amin ligandlarını birleştiren hibrit bir ligand stratejisi geliştirilmiştir. Çözelti içinde gerçekleştirilen ligand değişimi, farklı metal halojenür tuzları kullanılarak başlangıçtaki oleik asit ligandlarının etkin bir şekilde uzaklaştırılmasını sağlarken, NPL'lerin optik ve yapısal bütünlüğü korunmuştur. İncelenen ligandlar arasında, $(\text{NH}_4)_2\text{ZnCl}_4$ en etkili inorganik pasivasyonu sağlayarak halojenür ile muamele edilmiş örnekler arasında en yüksek ışımaya verimliliğine (%15) ulaşmıştır. Ardından uygulanan alkil amin işlemi, apolar çözücülerde kolloidal kararlılığı yeniden kazandırmış ve ışımaya verimliliğinin sentez sonrası oleik asit ligandlar ile kaplı NPL'lerin değerlerine yaklaşacak şekilde önemli ölçüde artmasını sağlamıştır (%60). Bu hibrit ligand yaklaşımı, kolloidal NPL sistemlerinde kompakt yüzey pasivasyonu, yüksek ışımaya verimliliği ve çözeltiyle işlenebilirliğin eş zamanlı olarak elde edilmesi için etkili bir yol sunmaktadır.

Research Article

10.65520/erciyesfen.1877955

Imprint:

Volume: 42(2)

Year: 2026

Page: 425-436

 Yusuf KELESTEMUR^{a*}

^a Asst. Prof., Middle East Technical University, yusufk@metu.edu.tr

* Corresponding Author

Received: 1/30/2026

Accepted: 4/20/2026

Citation:

Yusuf KELESTEMUR (2026). Hybrid Ligand Engineering for CdSe/CdS Core/Shell Colloidal Nanoplatelets. *Erciyes University Journal of Institute Of Science and Technology*, 42(2), 425-436.

<https://doi.org/10.65520/erciyesfen.1877955>

Screened by

 iThenticate[®]
for Authors & Researchers



Except where otherwise noted, content in this article is licensed under a Creative Commons 4.0 International license. Icons by Font Awesome.

Anahtar kelimeler: Kolloidal yarıiletken nanokristaller, Kolloidal nanolevhacıklar, Ligand değişimi, Optoelektronik malzemeler, İnorganik ligandlar



1. INTRODUCTION

Colloidal semiconductor nanocrystals have emerged as an important class of materials for optoelectronic applications owing to their size, shape, and composition tunable optical properties and electronic structures [1]. These nanocrystalline semiconductors exhibit narrow emission linewidths, high photoluminescence quantum yield (PLQY) and large absorption cross-sections, making them highly attractive for light-emitting applications [2]. These properties have enabled their widespread use in display technologies, particularly as color-converting films in liquid crystal displays (LCDs). In such photoluminescent-type display technologies, color-converting films employing green- and red-emitting nanocrystals are integrated with blue light-emitting diodes (LEDs) to achieve high brightness and wide color gamut [3]. While these developments clearly demonstrate the technological relevance of colloidal semiconductor nanocrystals, intrinsic limitations of LCD architectures, such as inefficient spectral utilization and limited contrast arising from continuous white backlighting, have motivated the exploration of electroluminescent, self-emissive display technologies [4].

At this stage, nanocrystal-based light-emitting diodes (NC-LEDs), in which colloidal semiconductor nanocrystals serve as the active electroluminescent layer, have attracted significant attention as promising alternatives [5, 6]. Since the first demonstration of NC-LEDs, substantial progress has been achieved through advances in nanocrystal synthesis, device architectures, and charge-transport layers, enabling external quantum efficiencies exceeding 20% across the visible spectrum [7]. Nevertheless, these impressive efficiencies are typically realized at relatively low operating voltages, while operational stability remains a critical challenge. Under prolonged operation or at high driving voltages, NC-LEDs often suffer from pronounced efficiency roll-off and limited device lifetimes, which continue to impede their commercial implementation [8].

One of the primary factors governing the efficiency and stability of NC-LEDs is the device architecture [7]. In particular, very high external quantum efficiency values have been achieved using hybrid device configurations that employ inorganic electron transport layers and organic hole transport layers. Zinc oxide nanoparticle-based electron transport layers have been widely adopted due to their favorable energy level alignment and high electron mobility; however, the substantial mismatch in charge carrier concentration and mobility between the inorganic and organic layers frequently leads to unbalanced charge injection at high operating voltages [9]. Excess electrons can accumulate at the interface between the emissive nanocrystal layer and the organic hole transport layer, accelerating interfacial degradation and enhancing nonradiative Auger recombination within the nanocrystals. As a consequence, NC-LEDs often exhibit efficiency degradation and compromised operational stability under practical operating conditions.

To mitigate these issues, extensive efforts have focused on controlling charge injection through materials and interface engineering. Early strategies primarily aimed to suppress electron injection using ultrathin insulating interlayers or doped metal oxide transport layers; however, these approaches often introduce additional drawbacks, including increased fabrication complexity, Joule heating, and reduced long-term stability [10, 11]. More recently, attention has shifted toward improving hole injection into the emissive layer via surface modification of colloidal nanocrystals. In particular, surface modification strategies employing metal halide salts have proven effective in passivating surface trap states, tuning energy band alignment, and improving charge transport in nanocrystal-based solar cells [12, 13]. More recently, similar strategies applied in nanocrystal-based

LEDs have further highlighted the central role of nanocrystal surface chemistry in governing optoelectronic behavior and overall device performance [14].

Although exciting results obtained from these studies, there are several problems with the commonly used ligand exchange approaches [13]. In the solid-state (in-film) ligand exchange strategies to introduce inorganic ligands into nanocrystal-based devices, pre-deposited nanocrystal films are exposed to ligand-containing solutions, enabling effective surface passivation and improved charge transport. However, solid-state ligand exchange can induce significant mechanical stress, volume contraction, and film cracking, particularly when long organic ligands are replaced by compact inorganic species. In addition, solvents used during in-film treatments may damage underlying functional layers, thereby limiting the applicability of this method in multilayer device architectures. As an alternative, in-solution ligand exchange has been widely explored for various nanocrystal systems. Despite its effectiveness in achieving inorganic surface passivation, this approach often renders surface-treated nanocrystals soluble only in highly polar solvents. Such solvents are generally undesirable for thin-film processing due to poor wetting behavior, high boiling points, and limited compatibility with common deposition techniques. Thus, these limitations highlight the need for surface engineering strategies that combine the advantages of inorganic passivation with the processability and film-forming properties of organic ligands.

To address these limitations from a materials perspective, two-dimensional colloidal nanoplatelets (NPLs) represent a particularly compelling platform due to their distinct optical properties and electronic structure [15]. Compared to conventional spherical nanocrystals, NPLs exhibit intrinsically narrow emission linewidths, suppressed nonradiative Auger recombination, and directional emission characteristics, making them highly attractive for light-emitting applications [16]. Moreover, when properly aligned, two-dimensional NPLs hold strong potential to surpass the performance of nanocrystal-based LEDs by enabling improved light outcoupling efficiency.

In this study, we employ CdSe/CdS core/shell NPLs as a model two-dimensional system for systematically investigating surface chemistry, as they offer several key advantages [17]. The relatively small lattice mismatch between the CdSe core and CdS shell enables uniform shell growth, leading to high PLQY. More importantly, the quasi-type-II band alignment results in partial delocalization of charge carriers across the core/shell interface, rendering the optical properties of these NPLs highly sensitive to surface modifications. This enhanced surface sensitivity makes them an ideal platform for investigating ligand-induced effects and amplifies the impact of surface engineering strategies compared to strongly confined spherical nanocrystals.

Building on this material platform and its strong sensitivity to surface chemistry, we developed hybrid strategy for CdSe/CdS core/shell NPLs, in which inorganic metal halide ligands and organic alkyl amine-based ligands coexist on the nanocrystal surface. Our hybrid ligand strategy involves an initial surface passivation using various metal halide salts, followed by a secondary treatment with alkyl amine ligands. This sequential modification preserves the benefits of halide-based passivation while restoring colloidal stability and enabling dispersion in chlorinated, nonpolar solvents suitable for thin-film processing. Notably, alkyl amine treatment not only improves processability but also leads to a significant enhancement in PLQY compared to the pre-exchange state.]

2. MATERIALS AND METHODS

2.1. Synthesis of colloidal semiconductor nanoplatelets. The synthesis of CdSe/CdS core/shell NPLs was performed via a two-step procedure following a previously reported method [18]. In the first step, four monolayer thick (4 ML) CdSe NPLs were synthesized and subsequently employed as seed for shell growth. The CdS shell was grown at elevated temperatures to promote high crystallinity. For a typical synthesis, 10 mL of octadecene (ODE) was loaded into a 100 mL three-neck

flask and degassed under vacuum at 100 °C for 1 h. The solution was then heated to 300 °C under a nitrogen atmosphere. Upon reaching 150 °C, cadmium and sulfur precursors, prepared as cadmium oleate (0.1 M in ODE) and octanethiol diluted in ODE (0.12 M), respectively, were continuously injected at a rate of 7 mL h⁻¹. After the injection of 0.5 mL of each precursor, CdSe core NPLs dispersed in degassed ODE were introduced into the reaction mixture. CdS shell growth was continued at 300 °C with further precursor injection (14 mL of each precursor), followed by an additional annealing step at the same temperature for 20 min. After annealing, the reaction was cooled to room temperature and the resulting CdSe/CdS core/shell NPLs were purified by successive precipitation and redispersion steps using hexane and ethanol to remove excess precursors and homogeneously nucleated CdS nanocrystals. The final purified NPLs were dispersed in hexane and stored for further ligand exchange studies.

2.2. Ligand exchange experiments. To obtain hybrid ligand-capped colloidal semiconductor NPLs, ligand exchange was performed using a two-step procedure. In the first step, the initially oleic acid capped CdSe/CdS core/shell NPLs were subjected to ligand exchange with inorganic ligands. For a typical ligand exchange, core/shell NPLs dispersed in hexane (10 mg/mL) were mixed with an N-methylformamide (NMF) solution containing metal halide salts (1 M). The resulting mixture formed a biphasic system and was vigorously mixed until complete phase transfer from the apolar hexane phase to the polar NMF phase was observed. This phase transfer indicates the successful replacement of oleic acid ligands with inorganic ligands, leading to NPLs dispersed in the polar NMF phase. After ligand exchange, the upper hexane phase was removed, and the polar phase containing the core/shell NPLs was washed several times with fresh hexane to remove residual organic ligands. The inorganic-ligand-capped NPLs were then precipitated by the addition of toluene and redispersed in fresh NMF.

2.3. Characterization. Absorption and photoluminescence (PL) spectra of colloidal NPLs were recorded using an Edinburgh Instruments FS5 spectrofluorometer. The PLQY of the samples was determined in solution using a Hamamatsu C11347 spectrometer. All measurements were carried out on NPLs obtained from the same synthesis batch to eliminate batch-to-batch variations. For each sample, PLQY was measured using multiple excitation wavelengths ranging from 400 to 500 nm in 10 nm intervals to account for absorption-dependent effects. The PLQY values were therefore evaluated over this excitation range and reported as intervals. Transmission electron microscopy (TEM) images were acquired with Hitachi HT7700 microscope operated at an accelerating voltage of 100 kV. Fourier-transform infrared (FTIR) spectroscopy measurements were performed using a Shimadzu IRTracer-100 spectrometer equipped with an attenuated total reflectance accessory, where the samples were drop-cast onto a diamond crystal.

2.4. Ethical Approval. Ethical approval is not required for this study.

3. RESULTS AND DISCUSSION

Two-dimensional colloidal NPLs were chosen due to their distinct optical properties and electronic structure [15]. Compared to conventional spherical nanocrystals, colloidal NPLs exhibit narrower emission linewidths, suppressed nonradiative Auger recombination, and intrinsically directional emission, making them particularly attractive for light-emitting applications [16]. In this study, CdSe/CdS core/shell NPLs were investigated as the model system. This material system is among the most extensively studied heterostructures in colloidal nanocrystals and offers several key advantages [17]. The relatively small lattice mismatch between the CdSe core and CdS shell enables uniform shell growth, leading to high PLQY. Moreover, the quasi-type-II like band alignment renders the optical properties of the resulting core/shell NPLs more sensitive to surface modifications, which is particularly advantageous for understanding surface-related effects through optical characterization.

First, 4 ML thick CdSe core NPLs were synthesized. The thickness of the CdSe NPLs was confirmed by absorption and PL spectroscopy, as shown in Figure 1a. The absorption spectrum of 4 ML thick CdSe NPLs exhibits two well-defined excitonic features located at approximately 480 and 512 nm, which are assigned to the heavy-hole and light-hole transitions. Consistent with these absorption features, the nanoplatelets exhibit a sharp photoluminescence emission peak centered at 513 nm with a full width at half maximum (FWHM) of only 8 nm, indicating a highly uniform thickness distribution and negligible inhomogeneous broadening. In addition to optical characterization, TEM analysis confirms the formation of rectangular-like CdSe NPLs with average lateral dimensions of 17.2×8.6 nm (Figure 1b).

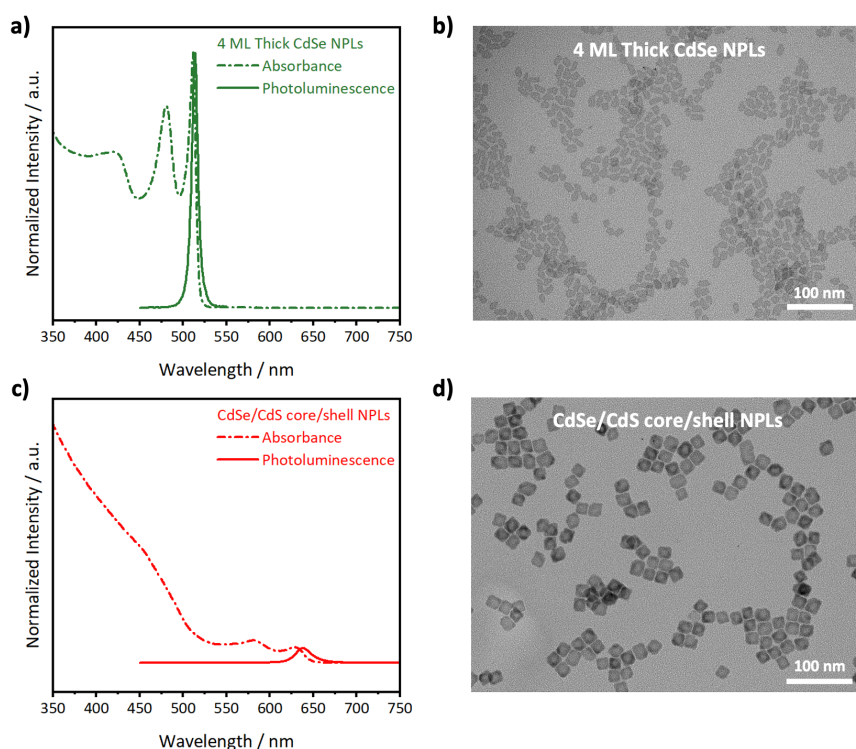


Figure 1. Optical and morphological characterization of the synthesized NPLs. Absorption and PL spectra of 4 ML thick CdSe NPLs (a) and CdSe/CdS core/shell NPLs (c). TEM images of 4 ML thick CdSe NPLs (b) and CdSe/CdS core/shell NPLs (d). Scale bars: 100 nm

In the second step, CdS shell growth was carried out at elevated temperature following a previously reported literature procedure [18]. Upon growth of the CdS shell, a pronounced red shift was observed in both the absorption and photoluminescence spectra of the resulting CdSe/CdS core/shell NPLs (Figure 1c). Specifically, the PL peak shifted to 638 nm. This substantial red shift can be attributed to the increased effective thickness of the core/shell structure, which leads to partial relaxation of quantum confinement. In addition to the spectral red shift, a noticeable broadening of excitonic features was observed. Compared to the very sharp emission of the core-only CdSe NPLs (FWHM of 8 nm), the FWHM of the CdSe/CdS core/shell NPLs increased to 22 nm. Such broadening is commonly attributed to enhanced exciton-phonon interactions in CdSe/CdS core/shell heterostructures, arising from increased structural complexity and carrier delocalization across the core-shell interface [19]. Furthermore, the absorption spectrum exhibits a pronounced enhancement in the short-wavelength region below 500 nm, indicating the contribution of the wide-bandgap CdS shell to the overall absorption. This observation provides further confirms the growth of CdS shell.

After the successful synthesis of CdSe/CdS core/shell NPLs, ligand exchange experiments were

carried out using a two-phase transfer approach. In a typical ligand exchange experiment, CdSe/CdS core/shell NPLs dispersed in n-hexane were mixed with an NMF solution containing the metal halide salts. During this process, the native organic ligands are replaced by metal halide species, rendering the NPLs dispersible in polar solvents and enabling phase transfer from the apolar to the polar medium. Initially, a range of metal halide ligands based on iodide, bromide, and chloride anions were investigated. However, in the case of iodide-based halide salts (CdI_2 , ZnI_2 , GaI_3 , MAICl_3 , MAZnI_3 , and NH_4I), complete phase transfer from the apolar n-hexane phase to the polar NMF phase was not achieved. Instead, the NPLs exhibited poor colloidal stability in the polar medium, leading to aggregation and precipitation. In contrast, metal bromide and chloride-based salts more effectively replaced the native oleic acid ligands on the surface of the CdSe/CdS core/shell NPLs, resulting in successful phase transfer.

The improved performance of chloride-based metal halide ligands compared to their iodide counterparts can be attributed to several factors [20, 21]. The smaller ionic radius of chloride ions provides a higher surface packing density and more homogeneous passivation for the flat surfaces of the NPLs. Furthermore, the interaction between cadmium and chloride ions exhibits favorable hard-soft acid-base (HSAB) compatibility, leading to more stable surface coordination. Reduced steric hindrance and faster binding kinetics of chloride ions further facilitate efficient replacement of native oleate ligands. In addition, the stronger solvation of Cl^- ions in polar NMF promotes stable dispersion of ligand-exchanged NPLs, whereas bromide- and iodide-based ligands often result in incomplete surface coverage and poor colloidal stability.

Absorption spectra of the ligand-exchanged CdSe/CdS core/shell NPLs capped with different chloride- and bromide-based halide ligands (CdCl_2 , ZnCl_2 , InCl_3 , NH_4Cl , $(\text{NH}_4)_2\text{CdBr}_4$, $(\text{NH}_4)_2\text{ZnBr}_4$, $(\text{NH}_4)_2\text{CdCl}_4$, $(\text{NH}_4)_2\text{ZnCl}_4$, MA_2CdBr_4 , and MA_2ZnBr_4) are presented in Figure 2. These NPLs yielded stable colloidal dispersions in polar media and revealed no significant changes in peak position or spectral linewidth, indicating that the ligand exchange process did not induce structural damage or etching of the surfaces of NPL. This observation is particularly important, as surface etching during ligand exchange is commonly associated with blue-shifted absorption features. Consistent with the absorption data, the PL spectra of the ligand-exchanged NPLs exhibited similar emission peak positions and FWHM, demonstrating good agreement between absorption and emission characteristics. Despite the preservation of the spectral features, a pronounced reduction in PLQY was observed after ligand exchange, with PLQY values decreasing from initial value of 52-61% to below 15%. Such behavior is commonly observed in colloidal nanocrystals capped with inorganic ligands and is generally attributed to incomplete surface passivation [20, 21].

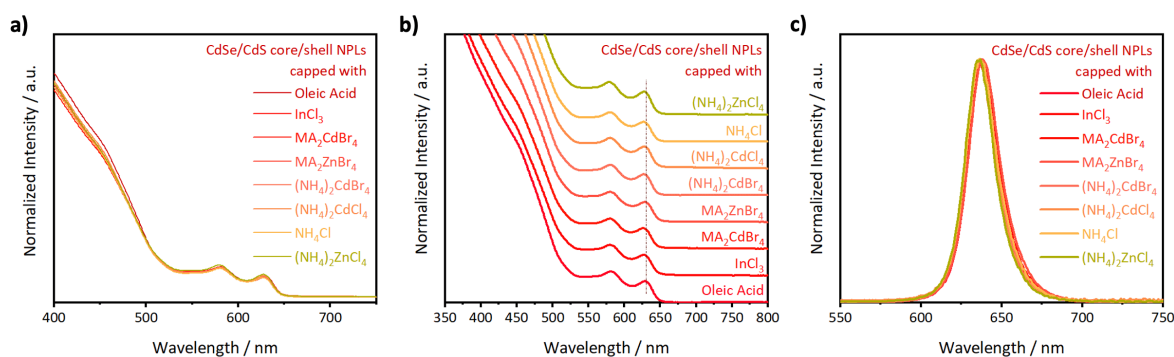


Figure 2. Optical characterization of CdSe/CdS core/shell NPLs before and after ligand exchange with different metal halide salts. Absorption spectra of CdSe/CdS core/shell NPLs shown in a stacked representation (a) and in an offset form (b) to facilitate direct comparison. PL spectra of CdSe/CdS core/shell NPLs capped with different ligands (c).

Among the investigated metal halide salts, $(\text{NH}_4)_2\text{ZnCl}_4$ yielded the highest PLQY, reaching approximately 14-19%. Consequently, this ligand system was selected for further studies. The comparatively higher efficiency observed with $(\text{NH}_4)_2\text{ZnCl}_4$ can be attributed to the presence of ZnCl_2 , which may function not only as an X-type ligand, analogous to oleic acid, but also as a Z-type ligand capable of coordinating undercoordinated surface atoms [22]. Moreover, zinc-based compounds are widely employed as shell materials, such as ZnS , to achieve effective surface passivation in colloidal nanocrystals. This intrinsic chemical compatibility is therefore expected to facilitate improved surface modification and account for the enhanced optical performance observed with ZnCl_2 containing ligand systems.

Morphological characterization of the colloidal NPLs was performed before and after the ligand exchange experiments. As shown in the TEM images in Figure 3, the lateral dimensions of the CdSe/CdS core/shell NPLs remain nearly unchanged following ligand exchange. This observation further corroborates the absence of any shift in the excitonic features observed in the absorption and photoluminescence spectra, indicating that the ligand exchange process does not induce morphological degradation or surface etching of the NPLs. Another notable feature observed in the TEM images is the change in the interparticle spacing of the core/shell NPLs. Prior to ligand exchange, oleic-acid-capped NPLs are well separated from each other, with interparticle distances largely determined by the length of the oleic acid ligands. In contrast, after ligand exchange, the core/shell NPLs exhibit pronounced aggregation and are frequently observed in direct contact with one another. This reduction in interparticle spacing is consistent with the replacement of long-chain organic ligands by significantly shorter inorganic ligands and therefore provides additional evidence for successful ligand exchange.

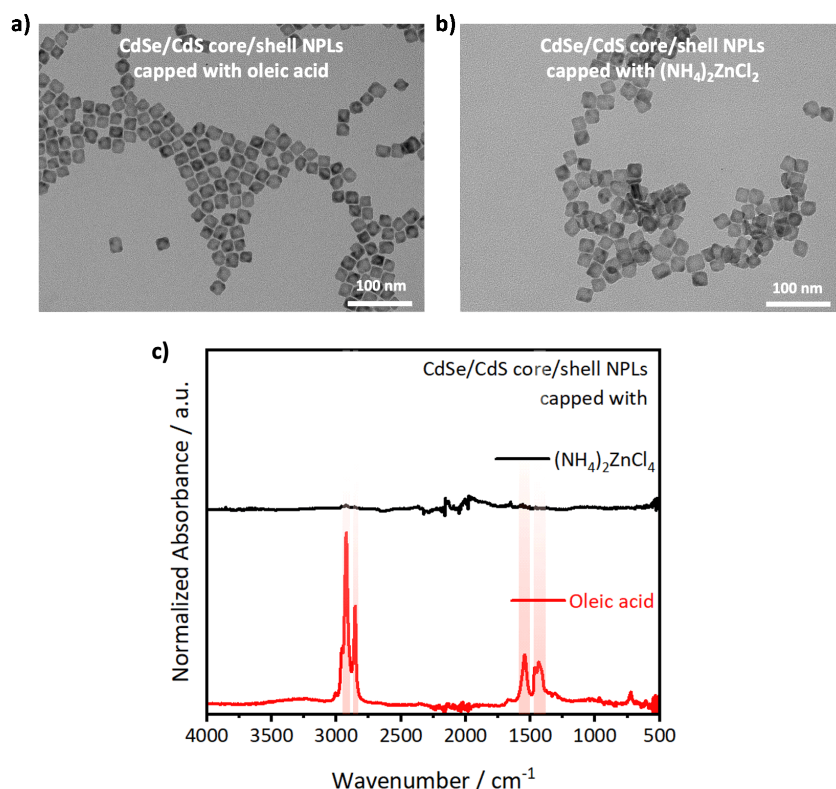


Figure 3. Morphological and surface chemical characterization of CdSe/CdS core/shell NPLs before and after ligand exchange. TEM images of CdSe/CdS core/shell NPLs capped with oleic acid (a) and capped with $(\text{NH}_4)_2\text{ZnCl}_4$ (b). Scale bars: 100 nm. Fourier transform infrared spectra of CdSe/CdS core/shell NPLs capped with oleic acid (c) and capped with $(\text{NH}_4)_2\text{ZnCl}_4$ (d).

Fourier transform infrared (FTIR) spectroscopy measurements were performed to further investigate the surface chemistry of CdSe/CdS core/shell NPLs and to verify the removal of organic ligands after ligand exchange. As shown in the FTIR spectrum of the as-synthesized core/shell NPLs, distinct vibrational features characteristic of oleic acid is observed, including the aliphatic C-H stretching modes and the carbonyl (C=O) stretching vibration. Following ligand exchange with metal halide salts, these characteristic vibrational modes disappear from the FTIR spectra, indicating the effective removal of oleic acid ligands and confirming successful inorganic ligand passivation of the nanoplatelet surface.

Following ligand exchange with metal halides, the resulting CdSe/CdS core/shell NPLs become dispersible in the polar NMF solvent. However, NMF is not compatible with common spin-coating processes due to its high boiling point, strong polarity, and slow evaporation rate, which hinder the formation of uniform thin films. Therefore, an additional surface modification step was required to transfer the inorganic-ligand-capped NPLs into a solvent compatible with solution-based film fabrication. To address this limitation, various alkyl amines, including butylamine, propylamine, octylamine, and oleylamine, were introduced into the NMF dispersions of inorganic-ligand-capped core/shell NPLs [21]. Upon the addition of alkyl amines, the NPLs flocculated and precipitated from the NMF solution. The precipitated nanoplatelets were subsequently redispersed in chloroform, a nonpolar solvent that is well suited for spin-coating processes.

As shown in Figure 4, the absorption and PL spectra of the CdSe/CdS core/shell NPLs exhibit no significant changes in peak position or spectral linewidth after the introduction of alkyl amines, indicating that the electronic structure of the NPLs remains unaffected. Notably, a substantial increase in PLQY was observed following alkyl amine treatment, with PLQY values nearly recovering to those of the as-synthesized oleic-acid-capped NPLs (around 53-61%). This enhancement suggests improved surface passivation arising from the formation of a hybrid ligand environment. Further analysis of the hybrid-ligand-capped core/shell NPLs reveals that the presence of mixed organic-inorganic ligands effectively suppress stacking and aggregation of nanoplatelets, as evidenced by TEM images (Figure 4). In addition, FTIR measurements performed after hybrid ligand formation exhibit characteristic vibrational features associated with alkyl amines, including the N-H bending (scissoring) mode observed at approximately $1550-1600\text{ cm}^{-1}$, along with C-H stretching vibrations in the $2850-2950\text{ cm}^{-1}$ region. These features confirm the successful attachment of alkyl amine ligands to the surface of the core/shell NPLs.

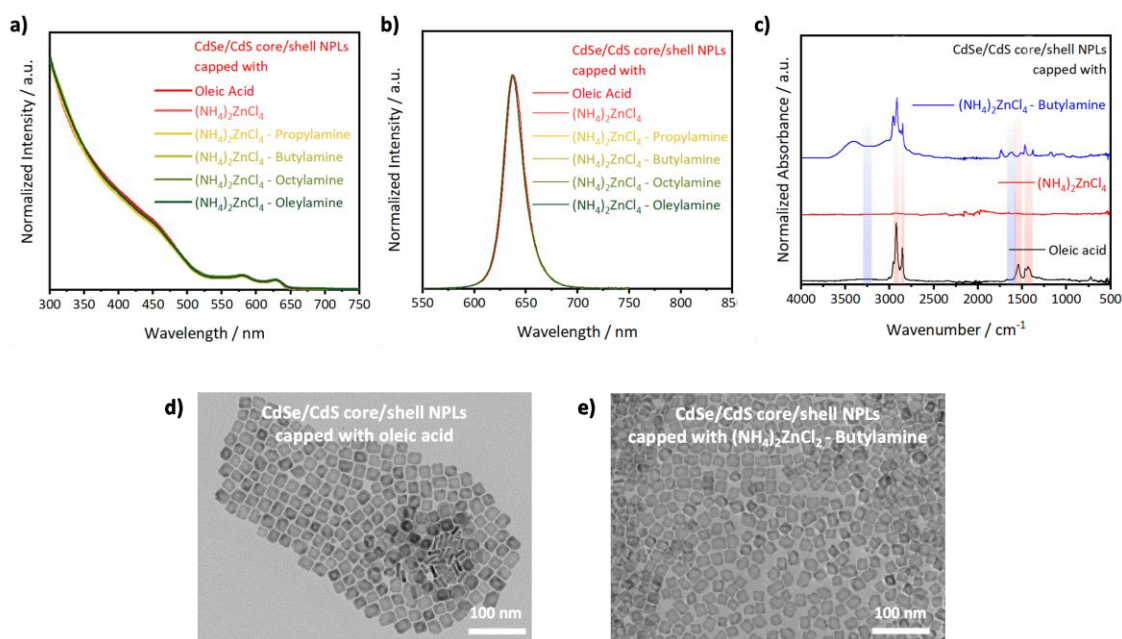


Figure 4. Optical and morphological characterization of hybrid ligand-capped CdSe/CdS core/shell NPLs. (a) Absorption, (b) PL and (c) FTIR spectra of CdSe/CdS core/shell NPLs capped with different hybrid ligands. (d) TEM image of CdSe/CdS core/shell NPLs capped with oleic acid and (e) $(\text{NH}_4)_2\text{ZnCl}_4$ -butylamine hybrid ligands. Scale bars: 100 nm.

4. CONCLUSION

The results demonstrate that surface chemistry plays a decisive role in controlling the optical performance and processability of CdSe/CdS core/shell NPLs. Metal halide ligands were deliberately employed as inorganic alternatives to long-chain organic ligands to achieve surface passivation while enabling processing in polar environments [20, 23]. These ligands can bind to the nanoplatelet surface through complementary X-type and Z-type coordination mechanisms. Specifically, halide anions act as X-type ligands by compensating positively charged surface metal sites, whereas metal halides such as ZnCl_2 can function as Z-type ligands by coordinating to chalcogen-rich or undercoordinated surface atoms [22]. This dual binding capability is particularly advantageous for core/shell NPLs, in which incomplete surface passivation readily introduces nonradiative recombination pathways. Among the investigated ligand systems, chloride-based ligands, especially ZnCl_2 containing salts exhibit enhanced effectiveness, consistent with their ability to establish more homogeneous and stable surface coordination.

Despite preserving structural integrity and excitonic features, purely inorganic ligand passivation leads to a substantial reduction in PLQY. This behavior is commonly observed in different colloidal semiconductor nanocrystals and attributed to incomplete surface passivation and the limited ability of rigid inorganic ligands to adapt to local surface heterogeneities. Importantly, the absence of spectral shifts or linewidth broadening confirms that this efficiency loss originates from surface electronic effects rather than structural damage. The introduction of alkyl amines as secondary ligands effectively resolves both efficiency and processing limitations [21].

The observed recovery in PLQY upon alkyl amine treatment can be understood in terms of the complementary roles of organic amines and inorganic metal halide ligands in surface passivation [21-23]. Alkyl amines, acting as L-type Lewis bases, can dynamically coordinate to undercoordinated surface metal sites, leading to partial passivation of surface trap states and a moderate increase in PLQY. In addition, amines may influence the surface stoichiometry and local coordination environment

by interacting with surface cations and modifying the ligand shell. However, amine ligands alone are generally insufficient to fully eliminate trap states, as they do not effectively passivate anionic surface sites that are primarily responsible for deep trap formation. In contrast, metal halide ligands, acting as Z-type Lewis acids, can strongly bind to undercoordinated surface anions, resulting in a significant reduction of nonradiative recombination pathways.

Within this framework, the hybrid ligand environment combines the advantages of both ligand types: inorganic metal halide species ensure effective passivation of anionic trap states, while alkyl amines contribute to additional passivation of cationic surface sites and improve the structural organization of the ligand shell. Furthermore, the presence of amines can facilitate the stabilization and redistribution of relatively weakly bound inorganic species at the nanocrystal surface, leading to a more uniform and consolidated passivation layer [21]. As a result, this synergistic interaction enables a more efficient suppression of surface traps, ultimately leading to the recovery of PLQY observed in hybrid ligand systems.

Our findings are consistent with ligand engineering strategies reported in the literature, where improved PLQY is achieved through hybrid ligand environments rather than purely inorganic surface treatments [22, 23]. In such systems, the presence of coordinating ligands alongside metal halide species is critical for maintaining effective and stable surface passivation, whereas purely inorganic ligand treatments often lead to reduced PLQY due to incomplete coverage or dynamic detachment from the nanocrystal surface [20].

In line with these reports, similar recovery of PLQY has been observed in spherical CdSe/CdS core/shell NCs upon sequential halide and amine treatment, where metal iodide salts were employed as the halide source [21]. While the overall behavior is consistent, our results suggest a possible dependence on nanocrystal geometry. In the case of NPLs, the atomically flat surface may impose stricter constraints on ligand packing, where larger halides such as iodide may not achieve sufficiently dense coverage. In contrast, smaller halides such as chloride may enable more effective surface packing and passivation, which could contribute to the improved optical performance observed in our system.

Overall, this work demonstrates that a rationally designed hybrid ligand strategy combining metal halide ligands with alkyl amines offers an effective route to achieve compact surface passivation, high PLQY and processing compatibility in colloidal NPLs systems. This approach provides a versatile platform for integrating NPLs into next-generation optoelectronic applications by using common solution processing steps. While this study is focused on material-level understanding of surface chemistry, the hybrid ligand approach developed here is expected to directly benefit device performance by improving charge transport and interfacial properties. The integration of these nanoplatelets into device architectures will be addressed in future work.



Peer-review: External, Independent.

Acknowledgements:

The author acknowledges the financial support provided by the TÜBİTAK Project-123E391 and the ODTÜ ADEP Project-11197.

Declarations:

1. Statement of Originality:

This work is original.

2. Author Contributions:

Concept: YK; **Conceptualization:** YK; **Literature Search:** YK; **Data Collection:** YK; **Data Processing:** YK;

Analysis: YK; **Writing – original draft:** YK; **Writing – review & editing:** YK.

3. Ethics approval:

Not applicable.

4. Funding/Support:

This work has not received any funding or support.

5. Competing Interests:

The author declares no competing interests.

6. GenAI Usage Statement:

No GenAI tools were used at any stage of the study.

7. Sustainable Development Goals:



REFERENCES

- [1] Talapin, D. v., Lee, J. S., Kovalenko, M. v., & Shevchenko, E. v. (2010). Prospects of colloidal nanocrystals for electronic and optoelectronic applications. *Chemical Reviews*, 110(1), 389–458.
- [2] Shu, Y., Lin, X., Qin, H., Hu, Z., Jin, Y., & Peng, X. (2020). Quantum dots for display applications. *Angewandte Chemie International Edition*, 59(50), 22312–22323.
- [3] Manders, J. R., Qian, L., Titov, A., Hyvonen, J., Tokarz-Scott, J., Acharya, K. P., Yang, Y., Cao, W., Zheng, Y., Xue, J., & Holloway, P. H. (2015). High efficiency and ultra-wide color gamut quantum dot LEDs for next generation displays. *Journal of the Society for Information Display*, 23(11), 523–528.
- [4] Kim, J., Roh, J., Park, M., & Lee, C. (2024). Recent advances and challenges of colloidal quantum dot light-emitting diodes for display applications. *Advanced Materials*, 36(20).
- [5] Wu, X., Ji, H., Yan, X., & Zhong, H. (2022). Industry outlook of perovskite quantum dots for display applications. *Nature Nanotechnology*, 17(8), 813–816.
- [6] Grim, J. Q., Manna, L., & Moreels, I. (2015). A sustainable future for photonic colloidal nanocrystals. *Chemical Society Reviews*, 44(16), 5897–5914.
- [7] Pietryga, J. M., Park, Y.-S., Lim, J., Fidler, A. F., Bae, W. K., Brovelli, S., & Klimov, V. I. (2016). Spectroscopic and device aspects of nanocrystal quantum dots. *Chemical Reviews*, 116(18), 10513–10622.
- [8] Moon, H., Lee, C., Lee, W., Kim, J., & Chae, H. (2019). Stability of quantum dots, quantum dot films, and quantum dot light-emitting diodes for display applications. *Advanced Materials*, 31(34).
- [9] Lim, J., Park, Y.-S., Wu, K., Yun, H. J., & Klimov, V. I. (2018). Droop-Free colloidal quantum dot light-emitting diodes. *Nano Letters*, 18(10), 6645–6653.
- [10] Dai, X., Zhang, Z., Jin, Y., Niu, Y., Cao, H., Liang, X., Chen, L., Wang, J., & Peng, X. (2014). Solution-

- processed, high-performance light-emitting diodes based on quantum dots. *Nature*, 515(7525), 96–99.
- [11] Zhang, Z., Ye, Y., Pu, C., Deng, Y., Dai, X., Chen, X., Chen, D., Zheng, X., Gao, Y., Fang, W., Peng, X., & Jin, Y. (2018). High-Performance, Solution-Processed, and Insulating-Layer-Free Light-Emitting Diodes Based on Colloidal Quantum Dots. *Advanced Materials*, 30(28).
- [12] Dirin, D. N., Dreyfuss, S., Bodnarchuk, M. I., Nedelcu, G., Papagiorgis, P., Itskos, G., & Kovalenko, M. v. (2014). Lead halide perovskites and other metal halide complexes as inorganic capping ligands for colloidal nanocrystals. *Journal of the American Chemical Society*, 136(18), 6550–6553.
- [13] Zheng, S., Chen, J., Johansson, E. M. J., & Zhang, X. (2020). PbS colloidal quantum dot inks for infrared solar cells. *iScience*, 23(11), 101753.
- [14] Kim, T., Kim, K.-H., Kim, S., Choi, S.-M., Jang, H., Seo, H.-K., Lee, H., Chung, D.-Y., & Jang, E. (2020). Efficient and stable blue quantum dot light-emitting diode. *Nature*, 586(7829), 385–389.
- [15] Lhuillier, E., Pedetti, S., Ithurria, S., Nadal, B., Heuclin, H., & Dubertret, B. (2015). Two-Dimensional colloidal metal chalcogenides semiconductors: synthesis, spectroscopy, and applications. *Accounts of Chemical Research*, 48(1), 22–30.
- [16] Kim, W. D., Kim, D., Yoon, D.-E., Lee, H., Lim, J., Bae, W. K., & Lee, D. C. (2019). Pushing the efficiency envelope for semiconductor nanocrystal-based electroluminescence devices using anisotropic nanocrystals. *Chemistry of Materials*, 31(9), 3066–3082.
- [17] Chen, O., Zhao, J., Chauhan, V. P., Cui, J., Wong, C., Harris, D. K., Wei, H., Han, H.-S., Fukumura, D., Jain, R. K., & Bawendi, M. G. (2013). Compact high-quality CdSe-CdS core-shell nanocrystals with narrow emission linewidths and suppressed blinking. *Nature Materials*, 12(5), 445–451.
- [18] Kelestemur, Y., Shynkarenko, Y., Anni, M., Yakunin, S., de Giorgi, M. L., & Kovalenko, M. v. (2019). Colloidal cdse quantum wells with graded shell composition for low-threshold amplified spontaneous emission and highly efficient electroluminescence. *ACS Nano*, 13(12), 13899–13909.
- [19] Antolinez, F. v., Rabouw, F. T., Rossinelli, A. A., Cui, J., & Norris, D. J. (2019). Observation of electron shakeup in cdse/cds core/shell nanoplatelets. *Nano Letters*, 19(12), 8495–8502.
- [20] Zhang, H., Jang, J., Liu, W., & Talapin, D. v. (2014). Colloidal nanocrystals with inorganic halide, pseudohalide, and halometallate ligands. *ACS Nano*, 8(7), 7359–7369.
- [21] Sayevich, V., Guhrenz, C., Dzhagan, V. M., Sin, M., Werheid, M., Cai, B., Borchardt, L., Widmer, J., Zahn, D. R. T., Brunner, E., Lesnyak, V., Gaponik, N., & Eychmüller, A. (2017). Hybrid N-Butylamine-Based ligands for switching the colloidal solubility and regimentation of inorganic-capped nanocrystals. *ACS Nano*, 11(2), 1559–1571.
- [22] Kirkwood, N., Monchen, J. O. v., Crisp, R. W., Grimaldi, G., Bergstein, H. A. C., du Fossé, I., van der Stam, W., Infante, I., & Houtepen, A. J. (2018). Finding and fixing traps in II-VI and III-V colloidal quantum dots: the Importance of Z-Type ligand passivation. *Journal of the American Chemical Society*, 140(46), 15712–15723.
- [23] Giansante, C. (2020). Library design of ligands at the surface of colloidal nanocrystals. *Accounts of Chemical Research*, 53(8), 1458–1467.

